Available online at www.sciencedirect.com
ScienceDirect
Tetrahedron 64 (2008) 1250–1256
Tetrahedron
www.elsevier.com/locate/tet

Morphological consequences of metal ion–peptide vesicle interaction

Surajit Ghosh, Prabhpreet Singh, Sandeep Verma*

Department of Chemistry, Indian Institute of Technology Kanpur, Kanpur 208016, Uttar Pradesh, India

Received 7 August 2007; received in revised form 2 November 2007; accepted 22 November 2007
Available online 24 November 2007

Abstract

The triskelion peptide conjugate **1**, having a Trp–Trp dipeptide unit on the three arms, was synthesized and studied for the interaction of peptide-based soft structures with metal ions, by fluorescence and microscopic analyses. We observed that fluorescence was significantly quenched upon addition of Cu(II) metal ions, whereas the addition of other metal ions also caused moderate to insignificant changes in the fluorescence emission, suggesting specificity of this triskelion peptide **1** for Cu(II) ions. The addition of Cu(II) and other metal ions also altered the morphology of preformed vesicles obtained from triskelion peptide **1** in a concentration-dependent fashion, as observed from microscopic analysis. Such metal-responsive soft structures may find potential use as novel materials for delivery and sensing applications.

1. Introduction

Peptide self-assembly follows the general design principles applicable for noncovalent syntheses of supramolecular architectures by invoking a variety of intermolecular interactions.[1] It involves hydrogen bonding and hydrophobic interactions, along with other possibilities, to build an array of complex, yet functional, motifs.[2] Of the possible molecular forces, aromatic π–π interactions play a central role in structure stabilization and are driven by side-chain interactions involving Trp, Phe and His residues.[3] Importantly, Gazit has proposed a role for aromatic amino acids in amyloid self-assembly, followed by the use of aromatic dipeptide motifs for the construction of peptide fibres and filaments.[4]

Fluorescence is an effective technique for the visualization and analysis of certain molecular recognition events, and in the present context, inherent fluorescence of the Trp indole chromophore and its sensitivity to local microenvironment may be used as a convenient probe to study metal ion–peptide interaction. Consequently, metal ion–indole interaction within the confines of the supramolecular association process and cation-dependent fluorescence changes were correlated with microscopic analysis.

We have recently reported an example of a synthetic triskelion peptide **1** (Fig. 1), containing a ditryptophan dipeptide around a tren scaffold, which afforded rapid self-assembly in solution, leading to the formation of vesicular structures.[5]

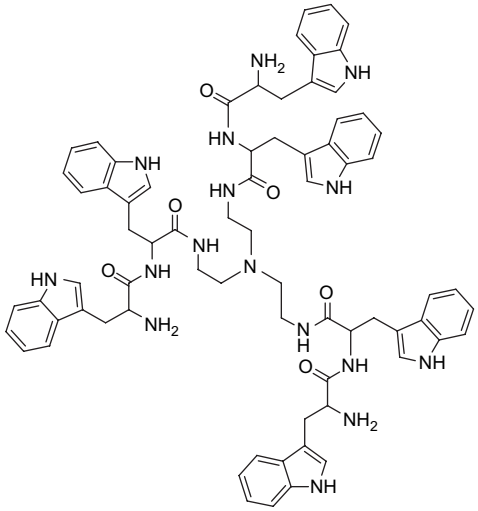

Figure 1. Molecular structure of triskelion peptide conjugate **1**.

* Corresponding author. Tel.: +91 512 259 7643; fax: +91 512 259 7436.
E-mail address: sverma@iitk.ac.in (S. Verma).

0040-4020/$ - see front matter © 2007 Elsevier Ltd. All rights reserved.
doi:10.1016/j.tet.2007.11.077

Rapid evolution and stability of such structures were primarily attributed to the favourable aromatic π–π interactions between tryptophan indole moieties. Owing to documented interactions of the Trp indole ring with Na^+, K^+ and Ca^{2+} ions,[6] we decided to study metal ion–peptide vesicle interaction with the objective of analyzing the ensuing effect(s) on ultrastructural morphologies of the vesicular structures.

2. Results and discussion

We decided to determine the binding stoichiometries of selected metal ions with preformed peptide vesicles. Compound **1** displayed a typical absorption peak at 275 nm, in the UV–vis spectrum, due to the Trp indole moiety and the spectral shape remained essentially the same without any spectral shift upon addition of Cu(II), but there was an increase in the absorbance with the incremental addition of 5 equiv of Cu(II).

In a preliminary fluorescence assay, the fluorescence of peptide conjugate **1** was screened in the presence of various metal ions and of the various candidates studied, Cu(II), Hg(II) and Ag(I) exhibited appreciable interaction with the preformed vesicles as determined from the extent of fluorescence quenching (Fig. 2). Addition of Cu(II) resulted in the most significant change—an observation well known for several Trp containing proteins. The observed quenching may be attributed to an electron transfer mechanism upon Cu(II) complexation to conjugate **1**.

Compound **1** exhibited an excellent specificity towards Cu(II) ions, when compared to other metal ions, in an experiment where several fold higher concentrations of other metal ions (50 μM) were added to the solution of **1** (1 μM) (Fig. 3). The fluorescence intensity was considerably quenched in the presence of copper ions (1 μM), while a change in fluorescence intensity was not observed for other metal ions.

Due to the pH dependence of **1**, the absorption and fluorescence emission spectra of **1** (1 μM) and effects of added equivalents of metal ions were carried out under constant pH conditions, i.e., CH_3OH/H_2O (1:1 v/v, 50 mM HEPES buffer, pH 7.0).

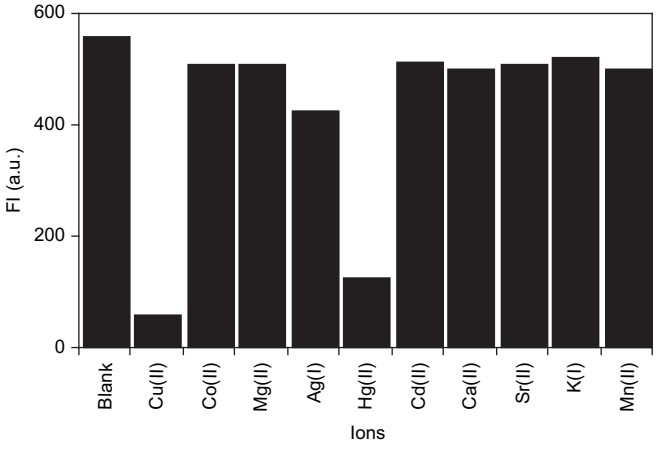

Figure 2. Fluorescence quenching of **1** (1 μM) by various metal ions (1 μM) in methanol/water (1:1).

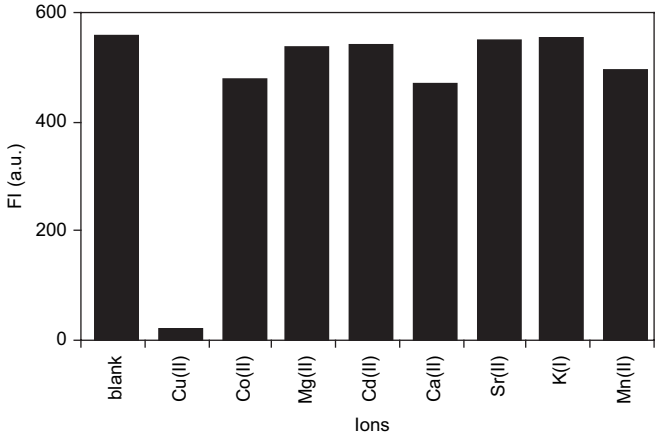

Figure 3. Comparative effects of copper (1 μM) versus other cations (50 μM) on **1** (1 μM).

The fluorescence emission intensity of **1** decreased gradually with the addition of copper ions in the concentration range of 0–2 μM.[7–9] A sharp linear decrease in intensity was evident till the addition of 0.5 μM of Cu(II), followed by a marginal decrease up to 1 μM and then a plateau was achieved (Fig. 4). These data suggest the presence of complexes other than 1:1 ratio. Spectral fitting of the fluorescence data through SPECFIT software revealed the formation of ML_2 and ML complexes with $\log \beta_{ML_2} = 14.5 \pm 0.19$ and $\log \beta_{ML}$=7.31±0.17, respectively. It is well documented that when Cu(II) binds tightly to a host compound, intracomplex quenching takes place (via *energy* or *electron* transfer).[8] Addition of excess EDTA to the assay mixture reversed the metal ion induced quenching.

Similarly, Hg(II) also caused sharp fluorescence quenching up to 2 μM (Fig. 5) of metal ion addition, followed by a plateau till 10 μM, thus indicating a 1:1 binding ratio. This suggests formation of ML complexes with $\log \beta_{ML}$=7.23±0.11. On the other hand, addition of Ag(I) ions resulted in fluorescence quenching till 10 μM (Fig. 6) followed by a marginal decrease till 20 μM, thus suggesting formation of both ML and M_2L complexes with $\log \beta_{ML}$=6.19±0.07 and $\log \beta_{M_2L}$ =

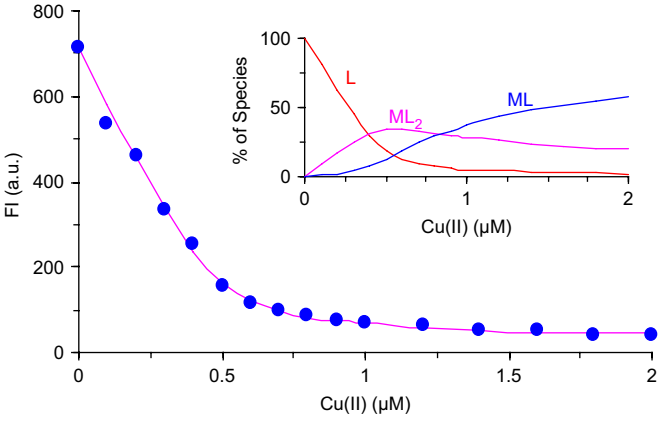

Figure 4. Fluorescence quenching of **1** (1 μM, λ_{em} 350 nm) in the presence of increasing concentrations of Cu(II) (0–2 μM) in CH_3OH/H_2O (1:1); inset: speciation diagram showing % distribution of ML_2 and ML species.

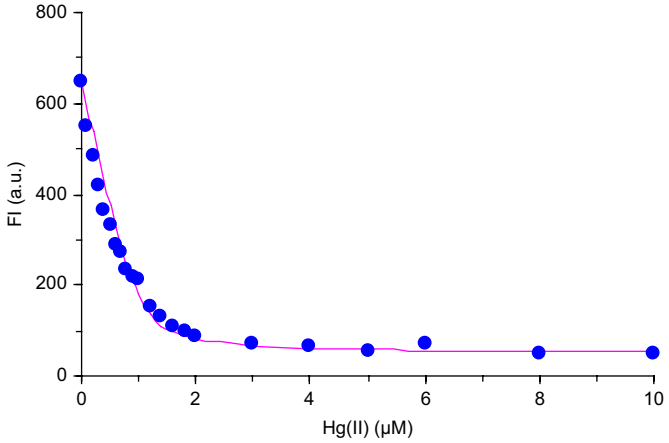

Figure 5. Fluorescence quenching of **1** (1 μM, λ_{em} 350 nm) in the presence of increasing concentrations of Hg(II) (0–10 μM) in CH_3OH/H_2O (1:1).

11.2 ± 0.15, respectively. For other metal ions viz., Co(II), Mg(II), Cd(II), Ca(II), Sr(II), K(I) and Mn(II), the fluorescence changes were insignificant and thus the log β values for these metal ions could not be calculated.

Fluorescence binding isotherms are indicative of a dramatic decrease in the fluorescence intensity of **1** in the presence of Cu(II) ions (<10% of initial values) when compared to Hg(II) and Ag(I) cations.

Interestingly, the addition of increasing amount of Ni(II) to **1** (1 μM), under similar assay conditions, suggested that a 50-fold higher concentration of Ni(II) is required to achieve the same changes as observed with Cu(II), thus revealing the higher sensitivity of **1** towards the latter metal ion (Fig. 7).

So, the triskelion peptide **1** showed good chelation towards the copper ion. It seems likely that the ligand **1** binds Cu(II) via nitrogens including one amide group of the dipeptide units. To determine the nature of the complex formed between **1** and Cu(II) in solution, we also carried out electrospray ionization mass spectrometry (ESI-MS) of the complex, which was obtained by dissolving metal and ligand in a 1:1 ratio under similar solvent condition as used in fluorescence studies followed by evaporation of the solvent. The signal obtained at

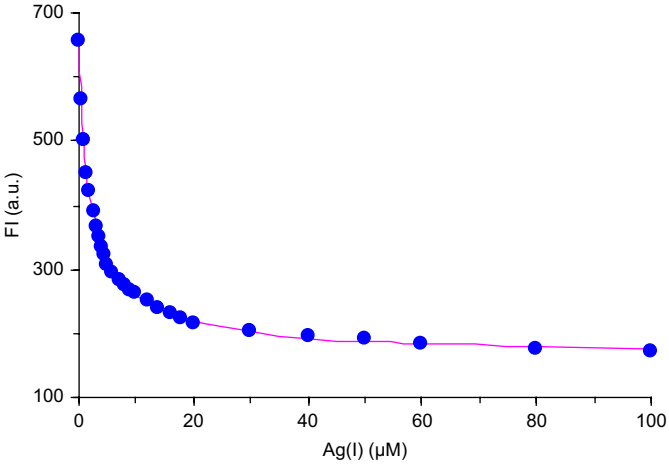

Figure 6. Fluorescence quenching of **1** (1 μM, λ_{em} 350 nm) in the presence of increasing concentrations of Ag(I) (0–100 μM) in CH_3OH/H_2O (1:1).

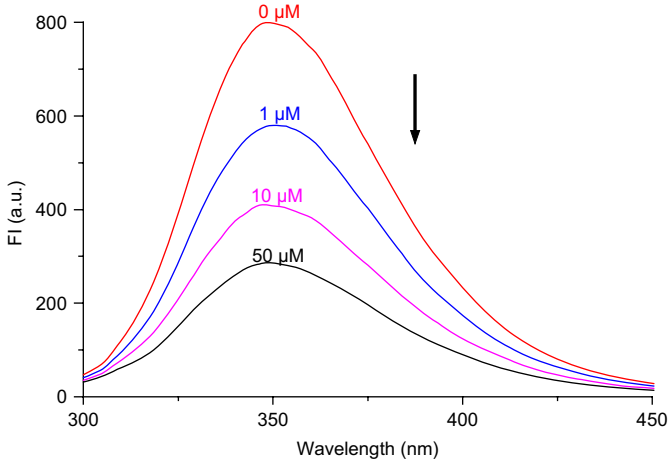

Figure 7. Fluorescence emission spectrum of **1** (1 μM) in CH_3OH/H_2O (1:1) with increasing concentration of Ni(II).

m/*z* unit of 1324.538 could be assigned to a species corresponding to $[M-2H+Cu]\cdot H^+$ along with isotopic distribution peak at 1326.543. The presence of a peak at *m*/*z* of 1263.625 is likely to be due to free peptide (MH^+) formed by decomplexation under ESI-MS condition. The involvement of the tertiary amino group in metal complexation is less likely (Figs. 8 and 9).

The other metals used, Ag(I) and Hg(II), are unable to interact with amide nitrogens and thus clear differences in binding are observed. On the basis of the present data available, it is not possible to assign a mechanism for Hg(II) quenching, either it shows quenching due to heavy atom effect thereby increasing the rate of intersystem crossing or may be it can bind to potential coordination site like endocyclic NH group of indole and oxygen atoms along with aromatic groups.[9]

Ag(I) is known to form stable bidentate complexes and occasionally tridentate or higher coordinate complexes in comparison with stabilization of octahedral complexes by other competing metal ions.[10] As the triskelion has a number of potential binding sites there is a possibility that one or more Ag(I) can interact with the same triskelion and result in the formation of ML and M_2L complexes. We also performed X-band EPR spectroscopy to investigate the mode of coordination of copper metal with conjugate **1**. EPR of copper (II)/

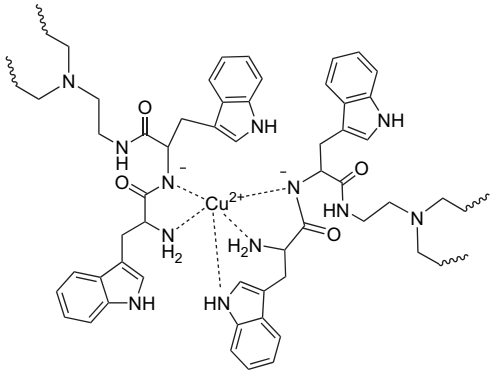

Figure 8. Possible mode of coordination for **1**/Cu(II) complex showing expected ML_2 formation. Only one arm containing dipeptide unit is shown for each ligand for clarity.

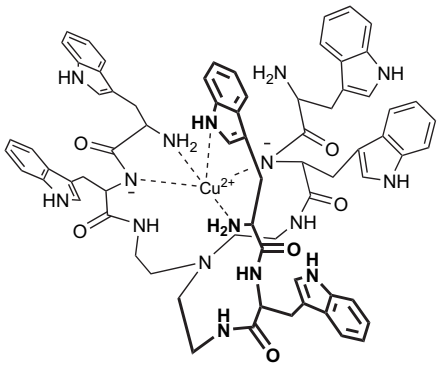

Figure 9. Possible mode of coordination for **1**/Cu(II) complex showing expected ML formation.

conjugate **1** in 50% aqueous methanol at room temperature showed isotropic spectra. However, at liquid nitrogen (120 K) temperature it showed an anisotropic spectrum with hyperfine splitting. We observed $g_{\|}$=2.39, $g_{\perp}$=2.078 G, $A_{\|}$=137 G signifying square pyramidal geometry around copper.

The fluorescence emission changes can be rationalized by considering the fact that Trp is located near metal ion binding site, thus complexation has significant effect on Trp emission properties. Metal ion–tryptophan interactions are extensively described in the literature.[11,12] Based on the premise that close contact between metal ion and Trp residue may have significant role on peptide vesicle structure, we decided to follow the morphological changes induced in preformed vesicles in the presence of metal ions.

Having reported extensively the solution phase self-assembly and morphology of peptide triskelion **1**, we became interested in determining the effect of metal ions on ultrastructural morphologies.

Interestingly, we also observed that interaction of peptide ligand **1** with transition metal ions such as Cu(II), Hg(II), Ni(II) and Ag(I) alters the morphology of the preformed vesicles of **1** in a concentration-dependent fashion. Minor changes in the shape of preformed vesicles[5] were observed after the addition of 25 μM Cu(II) ions (Fig. 10a and b). Further addition of Cu(II) ions crack opened the vesicular structures and made them leaky (Fig. 10c and d), thereby severely altering their morphology.[8] This observation confirmed that copper not only interacted with Trp indole and other possible sites in the vesicles, but also this interaction translated into a facile concentration-dependent morphing of soft structures.

Similarly we have checked the fate of the vesicles after interaction with other metal ions, Hg(II), Ni(II) and Ag(I). We have gradually increased the concentration of each metal ion followed by SEM imaging, and we observed complete disruption of the vesicular structures after addition of 3 mM Hg(II), 3 mM Ni(II) and 10 mM Ag(I) (Fig. 11a, b and d). It is interesting to note that the addition of certain ions such as potassium (3 mM) also resulted in the alteration of vesicular morphology (Fig. 11c). However, it had no effect in the fluorescence screening experiments. The quenching in the presence of Cu(II) and other metal ions demonstrates the interaction of the metal ion with ligand **1**. The fact that potassium and other metal ions do not quench the fluorescence is

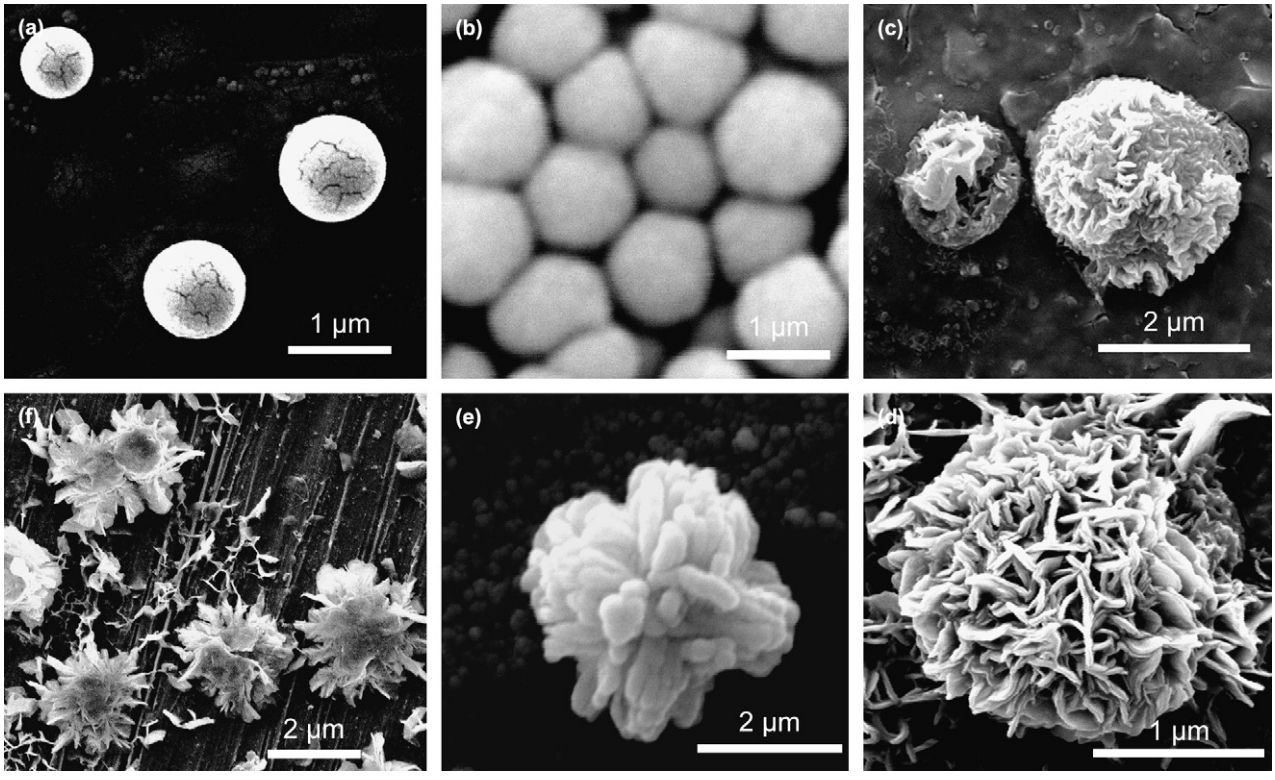

Figure 10. SEM micrograph of morphological changes in preformed peptide vesicles in the presence of Cu(II) ions. (a) Native vesicles; (b–f) after addition of 25, 50, 100, 250 and 300 μM Cu(II) ions, respectively.

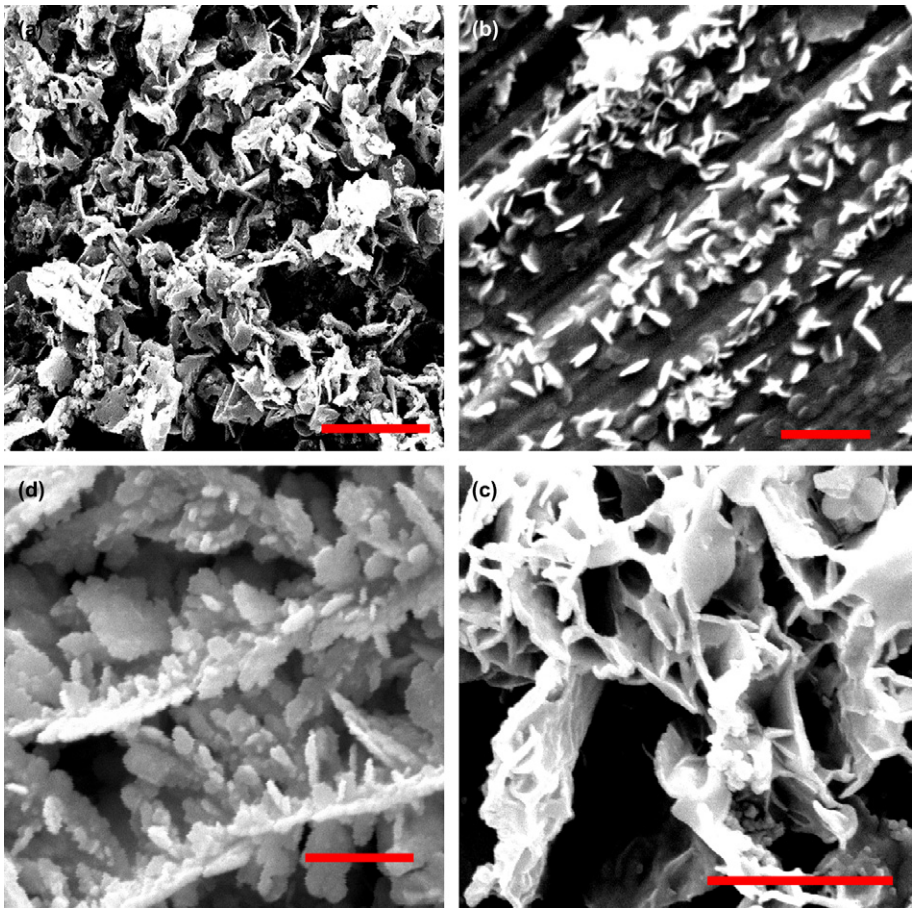

Figure 11. SEM micrograph of peptide vesicles upon addition of (a) Hg(II); (b) Ni(II); (c) K(I) and (d) Ag(I) ions. Scale bar corresponds to 5 μm.

not an indication of the absence of binding, because these metal ions do not usually interfere with fluorescence emission.

Morphological transformations were also determined by following the fate of rhodamine B filled vesicles using fluorescence microscopy. The rupture of well-formed spherical peptide structure was observed on metal ion addition (Fig. 12b–d). Direct interaction of metal ions causing attenuation of Trp fluorescence and morphological control of peptide-based soft vesicular structures may lead to interesting design paradigms. Such an approach may offer the possibility of peptide architectures, containing aromatic amino acids, which morph in the presence of selected metal ions. As suggested, this situation may also result from direct interaction of metal ion(s) with the aromatic nucleus, or at other sites. The present example follows the former mechanism, as we observe strong to marginal fluorescence quenching.

3. Conclusions

We have reported and demonstrated a unique example, where metal ion addition controls peptide vesicular morphology via direct interaction with the Trp indole, causing concomitant change in the fluorescence pattern. Such metal-responsive soft structures may find use as novel materials for a variety of delivery and metal sensing applications. Detailed studies concerning the mechanism of fluorescence quenching and the discriminatory behaviour of certain metal ions towards **1** are being carried out and will be reported in due course.

4. Experimental

4.1. Fluorescence and UV–vis studies

Fluorescence and absorption spectra were recorded on Perkin Elmer Luminescence spectrometer (LS 50B) and CARY 100 Bio UV–Vis spectrophotometer with a 1 cm quartz cell at 25±0.1 °C. The solutions of **1** and metal salts were prepared in CH_3OH/H_2O (50:50). Deionized water and methanol (analytical grade) were used in these studies. The solutions containing **1** (1 μM) and different concentrations of metal salts were prepared in HEPES buffer (50 mM), pH 7.0 and were kept at 25±1 °C for 2 h before recording their fluorescence spectra. All absorption and fluorescence scans were saved as ACS II files and further processed in Excel™ to produce all graphs shown.

*4.2. Determination of the binding constants of **1** towards metal ions*

The solution containing **1** (1 μM) in pH 7.0 buffer (HEPES 50 mM) was taken in a quartz cell and the absorbance or fluorescence spectrum recorded. The addition of different

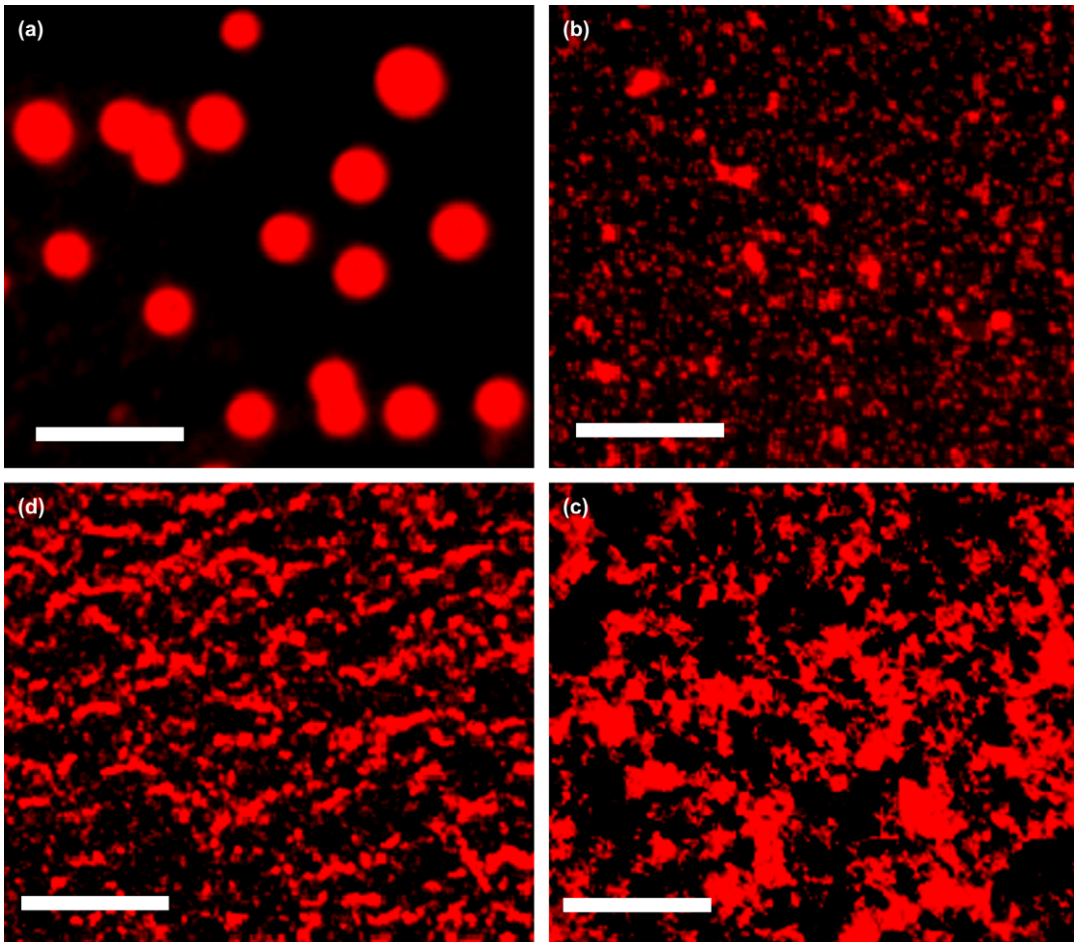

Figure 12. Fluorescence microscopic analysis of metal ion addition. (a) Rhodamine B loaded vesicles; (b–d) after addition of Cu(II), Hg(II), and Ag(I), respectively. Scale bar corresponds to 2 μm.

concentrations of metal nitrates was carried out with a micropipette in the intervals of 0.05–0.1 equiv in the same cell and each time the solution was allowed to stand for 3 min, before recording the absorbance or fluorescence spectrum. The spectra obtained were analyzed through curve fitting procedures using SPECFIT 3.0.36 (Demo Version) to determine the stability constants and distribution of various species. For calculation of binding constants for metal complexes using SPECFIT we applied the following equations for fitting our experimental data. For example, in the case of Cu(II) titration, for the formation of ML_2 complex we can write two stability constants as follows: $M+L \rightarrow ML$; $K_1=[ML]/[M][L]$ and $ML+L \rightarrow ML_2$; $K_2=[ML_2]/[ML][L]$, where K_1 and K_2 are stepwise stability constants. Alternatively we can write the overall stability constant as $M+2L \rightarrow ML_2$; $\beta=[ML_2]/[M][L]^2$ where $\beta=K_1 \cdot K_2$ and shows the overall stability constant for the complex ML_2. For the metal binding process, the stability constants (β) are reported as logarithmic values, i.e., log β value, a dimensionless quantity.

4.3. Fluorescence microscopy

Compound **1** (1 mM) was dissolved in 10 μM rhodamine B solution in 50% methanol/water and incubated for 2 days at 37 °C. After 2 days, 10 μL incubated solution was loaded onto the glass slide and followed by fluorescence microscopic imaging. These dye entrapped vesicular structures were examined on a fluorescent microscope (Zeiss Axioskop 2 Plus) provisioned with an illuminator (Zeiss HBO 100) and a rhodamine filter (absorption 540 nm/emission 625 nm). This filter optimized visualization of rhodamine-treated (positive resolution) compared with untreated (negative resolution) vesicles were virtually invisible in this light. Images were electronically captured utilizing Zeiss AxioVision (version 3.1). $CuCl_2 \cdot 2H_2O$ of 3 μM, 3 μM $HgCl_2$ and 10 μM of $AgNO_3$ solution were added to 2 days incubated dye entrapped vesicle solution. Ten microliters of each incubated solution (24 h) was loaded on glass slides, dried at room temperature and images taken under the microscope.

4.4. Scanning electron microscopy

A 20 μl aliquot of compound **1** was loaded onto the copper stubs and coated with gold. Various concentrations of $CuCl_2 \cdot 2H_2O$, $HgCl_2$ (3 mM), $NiCl_2$ (3 mM), KCl (3 mM) and $AgNO_3$ (10 mM) solutions were added to 2 days incubated vesicle solution. Ten microliters of the solution from each was loaded onto copper stubs and coated with gold, followed by scanning

electron microscopic imaging. SEM micrograph images were acquired using an FEI QUANTA 200 microscope equipped with a tungsten filament gun operating at WD 10.6 mm and 20 kV. Concentration of peptide sample was 1 mM.

Acknowledgements

S.G. thanks IIT Kanpur for a pre-doctoral fellowship. We thank Prof. V. Chandrasekhar and his group for allowing us to use their fluorescence setup. Prof. S. Ganesh is thanked for access to fluorescence microscope. This work is supported through a Swarnajayanti Fellowship in Chemical Sciences (DST) to S.V.

References and notes

1. (a) Lehn, J.-M. *Chem. Soc. Rev.* **2007**, *36*, 151–160; (b) Rapaport, H. *Supramol. Chem.* **2006**, *18*, 445–454; (c) Reinhoudt, D. N.; Crego-Calama, M. *Science* **2002**, *295*, 2403–2407.
2. (a) Zhao, X.; Zhang, S. *Macromol. Biosci.* **2007**, *7*, 13–22; (b) Fairman, R.; Aakerfeldt, K. S. *Curr. Opin. Struct. Biol.* **2005**, *15*, 453–463; (c) Zhao, X.; Zhang, S. *Trends Biotechnol.* **2004**, *22*, 470–476; (d) Rajagopal, K.; Schneider, J. P. *Curr. Opin. Struct. Biol.* **2004**, *14*, 480–486.
3. (a) Claessens, C. G.; Stoddart, J. F. *J. Phys. Org. Chem.* **1997**, *10*, 254–272; (b) Meyer, E. A.; Castellano, R. K.; Diederich, F. *Angew. Chem., Int. Ed.* **2003**, *42*, 1210–1250; (c) Waters, M. L. *Biopolymers* **2004**, *76*, 435–445.
4. (a) Reches, M.; Gazit, E. *Phys. Biol.* **2006**, *3*, S10–S19; (b) Reches, M.; Gazit, E. *Nano Lett.* **2004**, *4*, 581–585; (c) Reches, M.; Gazit, E. *Science* **2003**, *300*, 625–627; (d) Gazit, E. *FASEB J.* **2002**, *16*, 77–83.
5. Ghosh, S.; Meital, R.; Gazit, E.; Verma, S. *Angew. Chem., Int. Ed.* **2007**, *46*, 2002–2004.
6. (a) Aravinda, S.; Shamala, N.; Rajkishore, R.; Gopi, H. N.; Balaram, P. *Angew. Chem., Int. Ed.* **2002**, *41*, 3863–3865; (b) Hunter, C. A.; Lawson, K. R.; Perkins, J.; Urch, C. J. *J. Chem. Soc., Perkin Trans. 2* **2001**, 651–669; (c) Gallivan, J. P.; Dougherty, D. A. *Proc. Natl. Acad. Sci. U.S.A.* **1999**, *96*, 9459–9464; (d) Mcgaughey, G. B.; Gagne, M.; Rappe, A. K. *J. Biol. Chem.* **1998**, *273*, 15458–15463; (e) Burley, S. K.; Petsko, G. A. *Science* **1985**, *229*, 23–28; (f) Ghosh, S.; Singh, S. K.; Verma, S. *Chem. Commun.* **2007**, 2296–2298.
7. (a) Webb, M. A.; Loppnow, G. R. *J. Phys. Chem. B* **2002**, *106*, 2102–2108; (b) Masuda, H.; Sugimori, T.; Odani, A.; Yamauchi, O. *Inorg. Chim. Acta* **1991**, *180*, 73–79; (c) Tabak, M.; Sartor, G.; Neyroz, P.; Spisni, A.; Cavatorta, P. *J. Lumin.* **1990**, *46*, 291–299; (d) Li, Y.; Yang, C. M. *Chem. Commun.* **2003**, 2884–2885; (e) Zaric, S. D.; Popovic, D. M.; Knapp, E.-W. *Chem.—Eur. J.* **2000**, *6*, 3935–3942; (f) Filenko, A.; Demchenko, M.; Mustafaeva, Z.; Osada, Y.; Mustafaev, M. *Biomacromolecules* **2001**, *2*, 270–277; (g) Tabak, M.; Sartor, G.; Cavatorta, P. *J. Lumin.* **1989**, *43*, 355–361.
8. (a) Fabbrizzi, L.; Licchelli, M.; Pallavicini, P.; Perotti, A.; Sacchi, D. *Angew. Chem., Int. Ed. Engl.* **1994**, *33*, 1975–1977; (b) De Santis, G.; Fabbrizzi, L.; Licchelli, M.; Mangano, C.; Sacchi, D.; Sardone, N. *Inorg. Chim. Acta* **1997**, *257*, 69–76.
9. Corbeil, M.-C.; Beauchamp, A. L. *Can. J. Chem.* **1988**, *66*, 2458–2464; (b) Pesek, J. J.; Abpikar, H.; Becker, J. F. *Appl. Spectrosc.* **1988**, *42*, 473–477; (c) Chen, R. F. *Arch. Biochem. Biophys.* **1971**, *142*, 552–564; (d) Helene, C.; Toulme, J. J.; Le Doan, T. *Nucleic Acids Res.* **1979**, *7*, 1945–1954.
10. (a) Adam, K. R.; Baldwin, D. S.; Bashall, A.; Lindoy, L. F.; McPartlin, M.; Powell, H. R. *J. Chem. Soc., Dalton Trans.* **1994**, 237–238; (b) Fenton, R. R.; Ganci, R.; Junk, P. C.; Lindoy, L. F.; Lukay, R. C.; Meehan, G. V.; Prince, J. R.; Turner, P.; Wei, G. *J. Chem. Soc., Dalton Trans.* **2002**, 2185–2193; (c) Blake, A. J.; Gould, O. R.; Redek, C.; Schroder, M. *J. Chem. Soc., Chem. Commun.* **1994**, 985–986.
11. (a) Zhang, Y.; Cao, X.; Orbulescu, J.; Konka, V.; Andreopoulos, F. M.; Pham, S. M.; Leblanc, R. M. *Anal. Chem.* **2003**, *75*, 1706–1712; (b) Tang, B.; Niu, J.; Yu, C.; Zhuo, L.; Ge, J. *Chem. Commun.* **2005**, 4184–4186; (c) Torrado, A.; Walkup, G. K.; Imperiali, B. *J. Am. Chem. Soc.* **1998**, *120*, 609–610; (d) Zheng, Y.; Huo, Q.; Kele, P.; Andreopolos, F. M.; Pham, S. M.; Leblanc, R. M. *Org. Lett.* **2001**, 3277–3280.
12. (a) Weber, M. E.; Elliott, E. K.; Gokel, G. W. *Org. Biomol. Chem.* **2006**, *4*, 83–89; (b) Li, Y.; Yang, C. M. *J. Am. Chem. Soc.* **2005**, *127*, 3527–3530; (c) Hu, J.; Barbour, L. J.; Gokel, G. W. *New J. Chem.* **2004**, *28*, 907–911; (d) Gokel, G. W. *Chem. Commun.* **2003**, 2847–2852; (e) Schall, O. F.; Gokel, G. W. *J. Org. Chem.* **1996**, *61*, 1449–1458.